Systematic design of 2D and 3D VibroAcoustic Fluidic Cavity Sensors Using Topology Optimization

Belahurau, Yauheni; Aage, Niels; Christiansen, Rasmus Ellebæk; Lucklum, Frieder

Published in:
Proceedings of NOVEM 2023

Publication date:
2023

Document Version
Publisher's PDF, also known as Version of record

SYSTEMATIC DESIGN OF 2D AND 3D VIBROACOUSTIC FLUIDIC CAVITY SENSORS USING TOPOLOGY OPTIMIZATION

Y. Belahurau[1*], N. Aage[1,2], R. E. Christiansen[2], and F. Lucklum[1]

[1]Centre for Acoustic-Mechanical Microsystems (CAMM),
Technical University of Denmark (DTU), Ørsteds Plads 352, 2800 Kgs. Lyngby, DENMARK
[*]Email: yaube@dtu.dk

[2] Topology Optimization Group,
Technical University of Denmark (DTU), Nils Koppels Allé 404, 2800 Kgs. Lyngby, DENMARK

ABSTRACT

In this research we investigate a novel sensor concept, which utilizes a standing acoustic wave inside a liquid-filled cavity to probe volumetric properties of a fluid analyte. However, realizing a high-Q cavity resonator is a challenge because of low acoustic impedance contrast between liquids and solids. In our previous studies, we surround the cavity resonator with phononic crystal layers that provide a strong cavity resonance within the phononic band gap. The quality factor drastically depends on the geometry of the metamaterial lattice. Therefore, the main aim of this study is to find an optimal material layout of the solid domain around the cavity by employing topology optimization. We formulate the optimization problem as maximization of the Q-factor of the cavity resonance. We consider the sensor as a fully coupled vibroacoustic system, taking into account material losses and frequency-dependent material properties. Since resonance problems are very sensitive to minor variations in geometry, we apply a gray scale suppression constraint to minimize the influence of geometrical uncertainties and make the optimized designs suitable for additive manufacturing.

1 INTRODUCTION

A phononic-fluidic cavity sensor has first been demonstrated by Lucklum and Li [1] to measure volumetric properties of liquids, especially in volumes of 1 ml and less. A core element of the sensor is a liquid cavity resonator (LCR), which employs a standing acoustic wave inside to interact with a fluid analyte. A fluid cavity resonator of width w allows to estimate speed of sound of the liquid c directly by measuring the fundamental cavity resonance frequency $f_{res} = c/2w$. Consequently, the resonance frequency of the resonator is primerely sensitive

to changes in speed of sound as $\Delta f_{res} \propto \Delta c/2w$. In contrast to classic ultrasonic sensors, the LCR avoids a limitation in resolution in time-of-flight measurements with a short distance between the emitter and receiver. Furthermore, it provides a much longer interaction path for an acoustic wave in a liquid that results in higher sensitivity. Moreover, the interaction occurs within the bulk volume of the liquid and is not limited to a resonator surface unlike in acoustic resonant sensors such as, e.g. surface acoustic wave and quartz microbalance sensors [2, 3]. However, the practical usage of a LCR is difficult due to the low impedance mismatch between most liquids and solids that results in wide band resonance peaks. Thereby, in order to enhance a quality factor (Q-factor) of resonance peaks, the authors surrounded a cavity with phononic crystal layers.

A phononic crystal (PnC) is a subclass of acoustic metamaterials, which consists of a periodic arrangement of scattering centers in a surrounding matrix with a large acoustic mismatch [4]. The most appealing feature of a PnC is a capability to prevent propagation of elastic and acoustic waves in certain frequency ranges that are called band gaps. They appear due to Bragg scattering and local resonances. Thereby, band gaps can act as ideal reflectors to improve boundary conditions for cavity resonance, significantly increasing Q-factor and resolution. Moreover, we can localize acoustic resonance modes within a band gap that help to distinguish acoustic cavity and mechanical resonances clearly.

In order to find an optimal material layout around the LCR, we utilized the method of topology optimization. This method is developed by Bendsøe and Kikuchi [5] in 1988 to find the maximum stiffness material distribution for mechanical elements. By now, the method has proven its efficiency and is widely used in different application areas, e.g. in acoustics [6, 7], elastic wave propagation [8, 9] . Since a sensor is a fully-coupled vibroacoustic system, in our work we will use approaches that were suggested to design such types of problems [10].

2 SENSOR CONCEPT

To evaluate the transmission through a sensor element and to demonstrate its working principles, we established 2D and 3D coupled acoustic-mechanical finite element (FE) models using commercially available software COMSOL Multiphysics 6.0. Here, by transmission we assume the ratio between surface averaged velocity amplitudes at receiver and emitter respectively. In Fig. 1 we illustrated computational setups used for our study. In our models we applied periodic boundary conditions to liquid and solid boundaries perpendicular to wave propagation, in order to reduce a computational time. The PnC used in this work is based on a simple cubic cell with a spherical cutout. As the design parameters for a single unit cell, we consider the lattice constant a and the diameter of a spherical cutout d. In this study, we set a = 3 mm, the cavity width w = 2.5 mm. The cavity wall thickness can be expressed as $(a - w)/2$. For the 3D model we defined d = 1.3a and for the 2D models d = 0.9a, respectively. Contact with the emitter and receiver to excite and detect transmitted waves is modelled as a low-reflection impedance boundary condition with the effective transducer surface impedance of $2.1 \cdot 10^7 \frac{\mathrm{kg}}{\mathrm{m^2 s}}$. Moreover, we excite the emitter with a constant time-harmonic velocity amplitude of 0.1 m/s.

The model is meshed finely enough to capture the minimum wavelength encountered in this study. As a rule of thumb, this requires six elements per lattice constant (a). Thus, the maximum element size is set as $a/6$. The solid domain of the sensor is modeled as an acrylic plastic. In addition, we applied an isotropic loss factor to take account for material losses. For the fluid domain we utilize a viscous model taking into account bulk and dynamic viscosity. In order to demonstrate the sensor effect we use two liquids with 10% difference in speed of sound. Other material properties are the same. All material properties are summarized in Table 1.

Figure 2 demonstrates the computed transmission plots for 2D and 3D models. There are two clearly separated resonance peaks for the different liquids, with a frequency shift depending on

Table 1. Material properties for numerical analysis at 25 °C

	Acryl	Liquid 1	Liquid 2
Density (kg/m^3)	1186.4	1000	1000
Speed of sound (m/s)	-	1485	1633.5
Elastic modulus (GPa)	3.8	-	-
Isotropic loss factor	0.03	-	-
Dynamic viscosity (mPa·s)	-	1	1
Bulk viscosity (mPa·s)	-	2.47	2.47

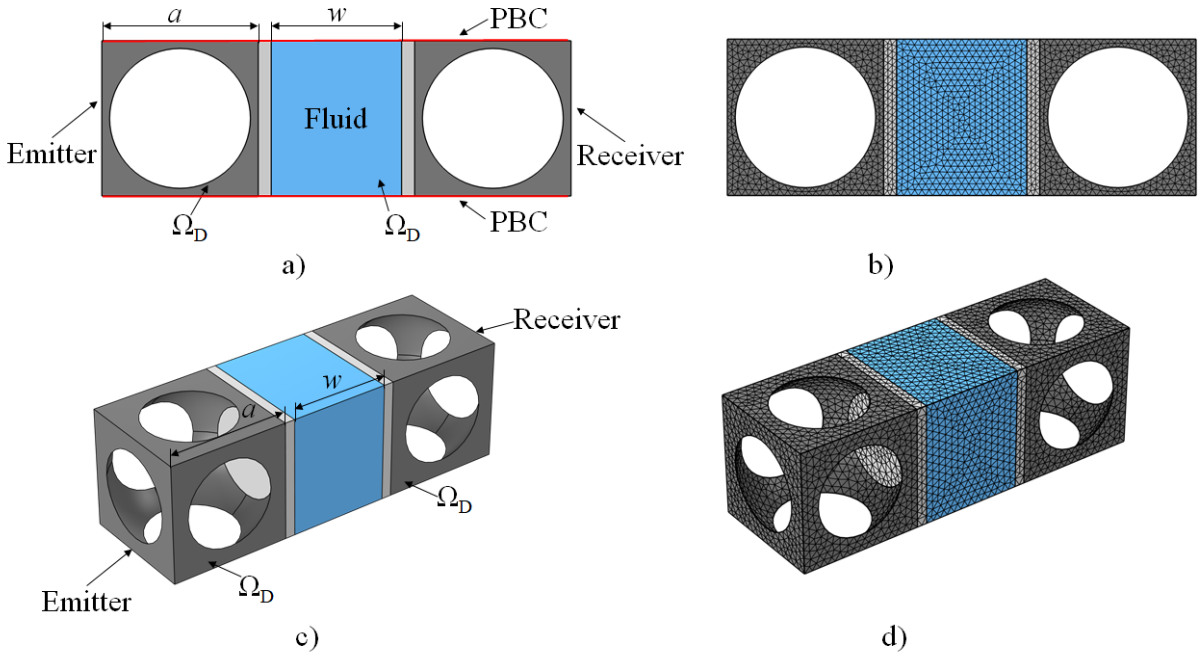

Figure 1: Computational models of phononic-fluidic sensor element with liquid domain (blue), cavity (light gray), PnC (dark gray) with boundary conditions for 2D setup (a) and its mesh (b), for 3D setup (c) and its mesh (d). Periodic boundary conditions are also applied to 3D model.

the change in speed of sound. The quality factor (Q) of resonance peaks can be calculated as $Q = f_r/\delta f$, where δf is the full width at half maximum of a resonance peak. The calculated Q-factor for the 2D design is 19 and for the 3D design is 61.

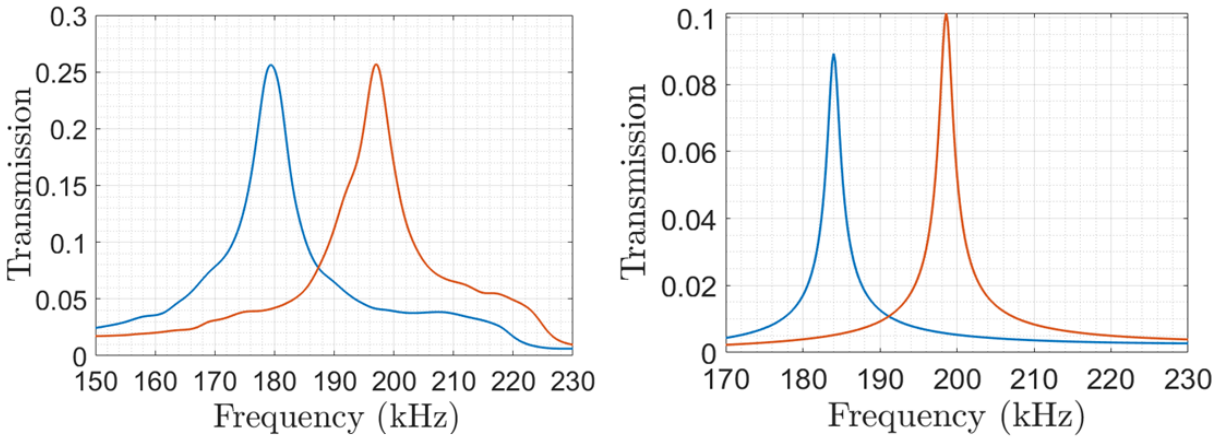

Figure 2: Frequency sweep through initial 2D (a) and 3D (b) designs. (Blue line corresponds to Liquid 1 and red line corresponds to Liquid 2).

3 OPTIMIZATION FORMULATION

The inverse design problem, solved by topology optimization, is formulated as a continuous, constrained optimization problem. Here, an objective function, approximating the quality factor by computing the transmission response for three frequencies, is defined along with a set of constraints. A continuous design variable field Θ is introduced to respresent the distribution of air (void) and solid material in the design domain. The element material property corresponds to air (void) and solid when $\Theta = 0$ and $\Theta = 1$ respectively. The objecitve function may be written as

$$Q = \frac{T(f_c)}{T(f_l) + T(f_r)} \tag{1}$$

where $T(f_c)$ is the transmission at central resonance frequency f_c, $T(f_l)$ and $T(f_r)$ are the transmissions at left f_l and right f_r of the full width at half maximum of a resonance peak respectively. To improve the algorithm's convergence towards a binary physically realizable design, a volume constraint, limiting the amount of solid material in the design domain is imposed. Moreover, we introduced a gray scale suppression constraint, limiting the fraction of the design field, Θ, taking intermediate values. The mathematical formulation of the optimization problem is may be written as

$$\begin{aligned} \max : \Phi &= \frac{T(f_c)}{T(f_l) + T(f_r)} \\ \text{subject to} : \frac{1}{\int_{\Omega_\mathrm{D}} dA} &\int_{\Omega_\mathrm{D}} \Theta dA - V_\mathrm{frac} \leq 0 \\ 4 &\int_{\Omega_\mathrm{D}} \Theta(1-\Theta) dA < \alpha_\mathrm{c} \end{aligned} \tag{2}$$

$\int_{\Omega_\mathrm{D}} dA$ is the area of the design domain Ω_D, the parameter $V_{frac} = 0.7$ represents the allowable fraction of structural material in the design domain and α_c is the fraction of gray area in the design domain. As a material interpolation scheme we used the so-called modified SIMP

approach [11] with a penalization factor of 3 and $\Theta_{min} = 10^{-5}$. To avoid mesh-dependent solutions we utilized a Helmholtz-type partial differential equation (PDE) filter [12]. The filter size $R_{\min}$ is $2\sqrt{2}h_{\max}$, where $h_{\max} = a/6$. Moreover, we employ thresholding [13] along with continuation of the thresholding strength β to the filtered design. For this study the thereshold level $\eta = 0.5$ is used. The threshold strength β is gradually increased from 2 to 16 and the gray scale suppression constant α_c is gradually decreased from 0.5 to 0.005 during the optimization process using a continuation scheme. The method of moving asymptotes (MMA) [14] is used in this work. Initial guess design is set to $\Theta = 1$. Thereby, solid material is gradually removed during the optimization process.

4 RESULTS AND DISCUSSION

4.1 2D Model

In Fig. 3a we present the design obtained after 120 iterations, Fig. 3b illustrates behaviour of the objective function during optimization. We can achieve Q-factor increase by seven times in contrast to the initial guess.The optimized design has the evident non-symmetry between left and right design domains due to the prescribed transducer impedance only at right boundary.

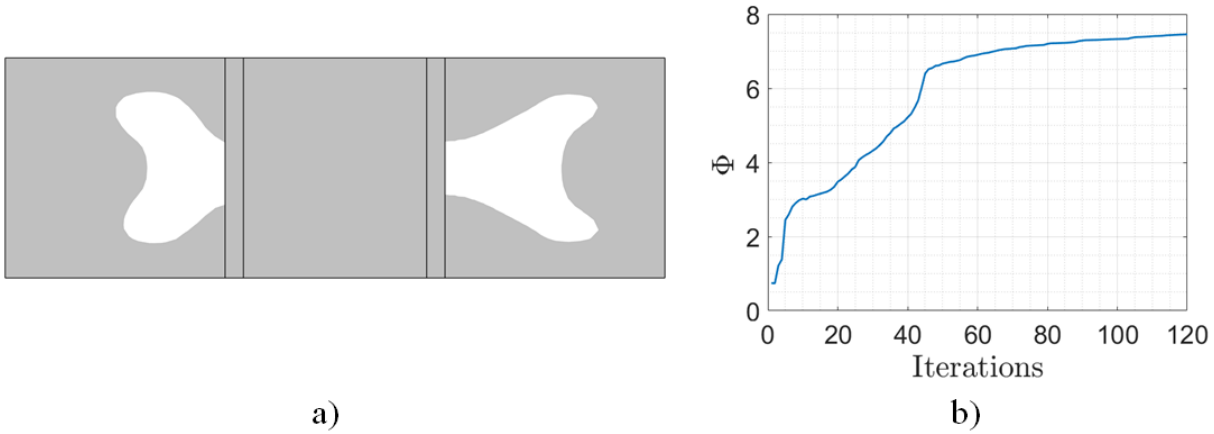

Figure 3: Optimized design of 2D phononic-fluidic sensor after 120 iterations (a) and evolution of objective function (b).

However, in order to make a relevant comparison with the reference design performance (see Fig. 2a), we had exported and remeshed again the optimized design and then performed a frequency sweep over the optimized design (see Fig. 4).

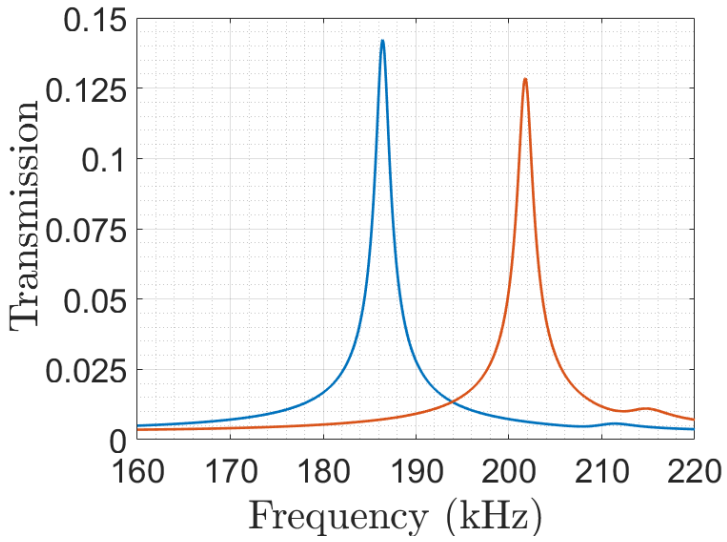

Figure 4: Transmission behavior of 2D optimized design (blue line corresponds to Liquid 1 and red line corresponds to Liquid 2).

The computed Q-factor of the first liquid is 86. Comparing this value with the Q-factor of the reference model (see Fig. 2a) we can conclude that the gain of the Q-factor is 4.5.

4.2 3D Model

Figure 5a shows the non-symmetry between left and right optimization domains, as in the previous case, due to the prescribed transducer impedance only at right boundary. Moreover, after 100 iterations we can achieve Q-factor increase by 60% in contrast to the initial guess. We also remeshed the optimized design to evaluate its transmission behaviour.

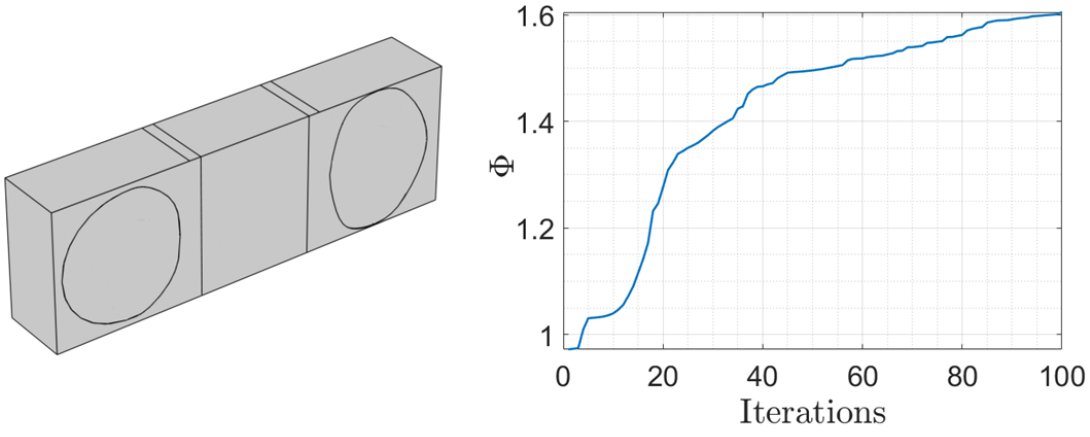

Figure 5: Optimized design of 3D phononic-fluidic sensor after 100 iterations (a) and evolution of objective function (b).

In this case, the computed Q-factor of the first resonance peak is 88 (see Fig. 6). Thereby, the gain of the Q-factor is 1.45 in comparison with the reference design (see Fig. 2b).

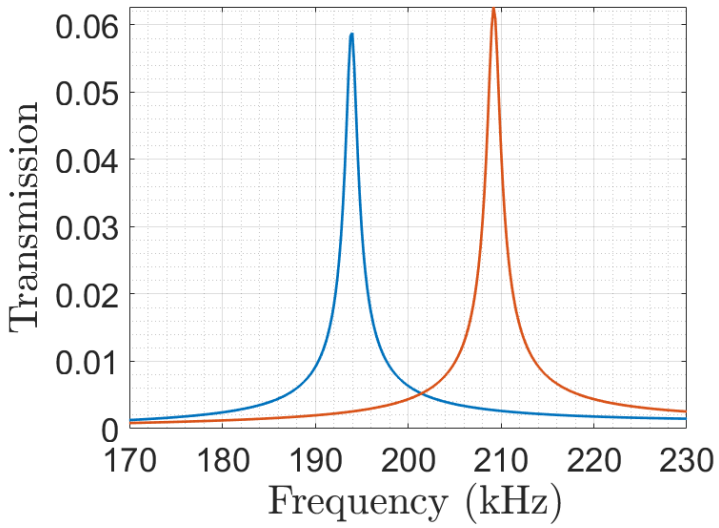

Figure 6: Transmission behavior of 3D optimized design (blue line corresponds to Liquid 1 and red line corresponds to Liquid 2).

To fabricate the optimized design we need to create a finite geometry based on the optimized semi-infinite model. Once the finite optimized model is ready and converted into a .STL file, we started doing test prints to be sure that the printed design is able to confine liquids without leakage. In this work we use a stereolitograpy (SLA) printer Asiga MAX UV35 with the pixel resolution of 62 μm and the minimal slice thickness of 35 μm. In order to characterize our samples, we measure the transmission between two wide-band longitudinal ultrasonic transducers (Olympus V-101-RM) with a center frequency of 500 kHz. The sensor element is clamped between the transducers using a coupling gel. Moreover, the transducer are placed on XYZ alignment stages.

5 CONCLUSIONS AND FUTURE WORK

We have presented selected results from our optimization studies. We demonstrated that topology optimization is a suitable tool to design a vibroacoustic phononic-fluidic cavity sensor. As a result of our study, we could increase a Q-factor by 4.5 times for the 2D case and 1.45 times for the 3D case. Since we consider a resonance optimization problem, our results strongly depend on the initial guess. In order to obtain a robust design of the sensor, our future work will implement additional approaches such as a double filtering technique. Ultimately, we apply multimaterial schemes and eigenvalue optimization approaches to find unique and robust designs, which are subsequently converted into designs suitable for additive manufacturing and validated by measurements.

ACKNOWLEDGEMENTS

Support by the Deutsche Forschungsgemeinschaft (DFG, German Research Foundation) under grant LU 2264/2-1 is gratefully acknowledged. Also we thank DTU Computing Center (DCC) for providing us access to the HPC.

REFERENCES

[1] R. Lucklum and J. Li. Phononic crystals for liquid sensor applications. *Meas. Sci. Technol.*, 20(124014), 2009.

[2] B. Jacoby and M. J. Vellekoop. Physical sensors for liquid properties. *IEEE Sens. Journ.*, 11(12):3076 – 3085, 2011.

[3] A. Mujahid and F. L. Dickert. Surface acoustic wave (saw) for chemical sensing applications of recognition layers. *Sensors*, 17(12):2716, 2017.

[4] P. A. Deymier. *Acoustic metamaterials and Phononic Crystals*. Berlin: Springer-Verlag, 2013.

[5] M. P. Bendsøe and N. Kikuchi. Generating optimal topologies in structural design using a homogenization method. *Comp. Meth. in Appl. Mech. and Eng.*, 71(2):197–224, 1988.

[6] O. Sigmund M. B. Dühring, J. S.Jensen. Acoustic design by topology optimization. *J. Sound and Vib.*, 317(3-5):557–575, 2008.

[7] E. Wadbro and M. Berggren. Topology optimization of an acoustic horn. *Comp. Meth. in Appl. Mech. and Eng.*, 196(13):420–436, 2006.

[8] J. S.Jensen. Topology optimization problems for reflection and dissipation of elastic waves. *J. Sound and Vib.*, 301(1-2):319–340, 2007.

[9] M. Schevenels B. S. Lazarov G. Lombaert C. van Hoorickx, O. Sigmund. Topology optimization of two-dimensional elastic wave barriers. *J. Sound and Vib.*, 376:95–111, 2016.

[10] O. Sigmund G. H. Yoon, J. S. Jensen. Topology optimization of acoustic–structure interaction problems using a mixed finite element formulation. *Int. J. Numer. Meth. Engng.*, (70):1049–1075, 2003.

[11] O. Sigmund. Morphology-based black and white filters for topology optimization. *Struct Multidisc Optim.*, (33):401–424, 2007.

[12] B. S. Lazarov and O. Sigmund. Filters in topology optimization based on helmholtz-type differential equations. *Int. J. Numer. Meth. Engng.*, (86):765–781, 2011.

[13] B. S. Lazarov F. Wang and O. Sigmund. On projection methods, convergence and robust formulations in topology optimization. *Struct Multidisc Optim.*, (43):767–784, 2011.

[14] K. Svanberg. The method of moving asymptotes – a new method for structural optimization. *Int. J. Numer. Meth. Engng.*, (24):359–373, 1987.